Prompt Fission Neutron Spectra of ^{235}U above emissive fission threshold

V.M. Maslov[1],N.V. Kornilov[2] , A.B. Kagalenko[2], N.A. Tetereva[1]
[1]Joint Institute of Nuclear and Energy Research - "Sosny", 220109, Minsk, Belarus
[2]Institute of Physics and Power Engineering, Obninsk, Russia

Abstract

Prompt fission neutron spectra from neutron-induced fission of ^{235}U at E_n ~7 MeV and E_n ~ 14.7 MeV are analyzed. Exclusive spectra of the pre-fission (pre-saddle) (n,$x$nf) reaction neutrons are calculated with Hauser-Feshbach statistical model, fission and (n,xn) reaction cross section data being described consistently. Observed prompt fission neutron spectra of ^{235}U are shown to be strongly correlated with the emissive fission contributions to the observed fission cross sections.

1 Introduction

The shape of the prompt fission neutron spectra (PFNS) of actinide neutron-induced fission much depends on the incident neutron energy E_n and the target nuclide fissility. In the domain of emissive fission reaction, the spectrum shape variation is defined mostly by the increase of the pre-fission neutron emission with increase of the E_n. Analysis of measured ^{238}U(n,F) and ^{232}Th(n,F) PFNS data showed that a number of data peculiarities could be correlated with the influence of (n,$x$nf) prefission neutron spectra on the observed PFNS [1, 2, 3]. Recent experimental investigations of PFNS of ^{235}U(n,F) by Ethvignot et al. [4] for E_n from 0.4 MeV up to 200 MeV, along with detailed PFNS data by Boykov et al. [5, 6] at E_n ~14.7 MeV provides a possibility to evidence the emissive fission influence on the PFNS for a wider range of excitation energies and fission probabilities.

2 MODEL

In a neutron-induced fission of ^{235}U at least two prompt fission neutron sources could be distinguished, namely: pre-fission and post-fission neutrons. Contribution of the pre-equilibrium neutron emission, which could be emitted before a composite nuclide ^{236}U attains thermal equilibrium, could be reliably fixed by the consistent description of ^{235}U(n,F), ^{235}U(n,2n) and ^{235}U(n,3n) reaction cross sections. Emission probability of the pre-fission neutrons, which might be evaporated before a composite system attains saddle-point deformation, is also fixed rather unambigously, because fission probabilities of ^{235}U and ^{234}U, emerging after successive emission of pre-fission (or pre-saddle) neutrons are defined by the description of ^{234}U(n,f) and ^{233}U(n,f) first-chance fission cross sections. Calculated exclusive (n,$x$nf) reaction neutron spectra for the ^{235}U+n interaction are strictly correlated with the consistent description of ^{235}U(n,F), ^{235}U(n,2n), ^{235}U(n,3n), ^{235}U(n,n') and ^{235}U total cross sections.

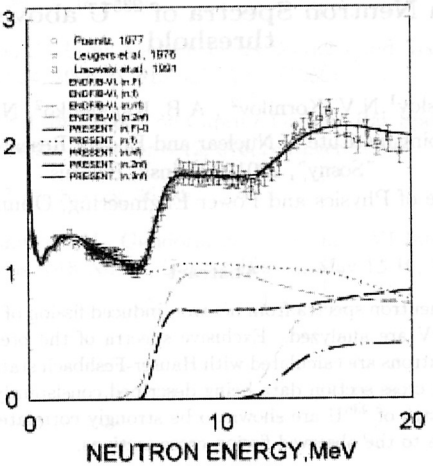

Figure 1: ^{235}U(n,F) cross section.

After scission neutrons are emitted by the primary fission fragments. The average energy of the prompt fission neutron spectrum $\langle E \rangle$ in the laboratory system (LS) is estimated as $\langle E \rangle = \langle \varepsilon \rangle + E_v$, where $\langle \varepsilon \rangle$ is the average neutron energy in the center-of-mass system (CMS) and E_v is the CMS energy per nucleon. Most of the neutrons are emitted from the fragments after full acceleration in their mutual Coulomb field, though it might be assumed that some neutrons could be emitted just after scission [7], i.e., before full acceleration of the fission fragments. This peculiarity was taken into account implicitly in modelling the PFNS of ^{232}Th(n,F) and ^{238}U(n,F) by decreasing the value of E_v.

2.1 Pre-fission (n,xnf) spectra

In case of ^{235}U(n,F) reaction at E_n ~14.7 MeV, i.e. above (n,2nf) reaction threshold E_{n2nf}, the contribution of (n,nf) and (n,2nf) reaction neutrons might be evidenced in PFNS [5, 6]. Contributions of (n,$x$nf) fission reactions to the observed (n,F) reaction cross section, coming from fission of relevant equilibrated U nuclei, are calculated in a Hauser-Feshbach approach, implemented in a STAPRE statistical model code [8] as

$$\sigma_{nF}(E_n) = \sigma_{nf}(E_n) + \sum_{x=1}^{X} \sigma_{n,xnf}(E_n), \tag{1}$$

using fission probabilities $P_{fi}^{J\pi}(U)$ of relevant nuclei

$$\sigma_{n,xnf}(E_n) = \sum_{J\pi} \int_0^{U_{x+1}^{maax}} W_{x+1}^{J\pi}(U) P_{f(x+1)}^{J\pi}(U) dU. \tag{2}$$

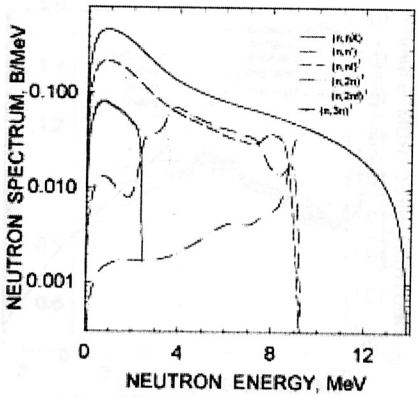

Figure 2: 1st neutron spectrum of ^{235}U(n,F) at 14.7 MeV

Here, $W^{J\pi}_{x+1}(U)$ is the population of $(x+1)-$th residual nucleus at excitation energy U after emission of x neutrons, excitation energy U^{max}_{x+1} is defined by the incident neutron energy E_n and the energy, removed from the composite system by (n,$x$nf) reaction neutrons. The other details are described elsewhere [2, 3].

Fission cross section data of ^{235}U(n,F) are compared with the calculated curve on Fig. 1. The contributions of x-th multiple-chance fission reactions to the observed fission cross section $\beta_x(E_n) = \sigma_{n,xnf}(E_n)/\sigma_{nF}(E_n)$ and exclusive pre-fission neutron spectra $d\sigma^i_{n,xnf}/d\varepsilon$, $i = 1...x$, were calculated simultaneously. Observed fission cross section data [9, 10] for ^{235}U(n,F) reaction and contributions of the ^{235}U(n,f) (first-chance) fission reaction, ^{235}U(n,nf) (second-chance) fission reaction and ^{235}U(n,2nf) (third-chance) fission reactions to the observed ^{235}U(n,F) fission cross section are shown on Fig. 1. For $E_n > E_{nnf}$, first-chance (non-emissive) fission cross section of ^{235}U(n,f) is rather weak function of E_n, it is similar to the trends, predicted for ^{238}U(n,F) and ^{232}Th(n,F) reactions [2, 3, 11]. Present multiple fission chances partitioning of the observed ^{235}U(n,F) fission cross section is strongly discrepant with the predicted fission chances distribution of ENDF/B-VI [12]. We argue that estimates of multiple-chance fission contributions, different from that shown on Figs. 1, would either deteriorate consistent description of ^{235}U(n,F), ^{235}U(n,2n) and ^{235}U(n,3n) or non-emissive ^{234}U(n,f) and ^{233}U(n,f) reaction cross sections.

Present statistical model of fission reaction assumes fission/neutron evaporation competition during decay of the excited compound nucleus, which is formed after the first-chance emission of pre-equilibrium neutron [8], treated with a simple version of exciton model [14, 15]. The equilibration is treated with a set of master-equations, describing the evolution of the excited nucleus states, classified by the number of particles plus holes [8]. Equations, used to calculate the exclusive pre-fission neutron spectra are described elsewhere [2, 3]. For example, exclusive neutron spectrum of the first neutrons $\frac{d\sigma^1_{n2nf}}{d\varepsilon}$ of (n,2nf)^1 reaction, i.e. ^{235}U(n,2nf)^1, is obtained integrating the first neutrons spectrum of ^{235}U(n,2nx) reaction,

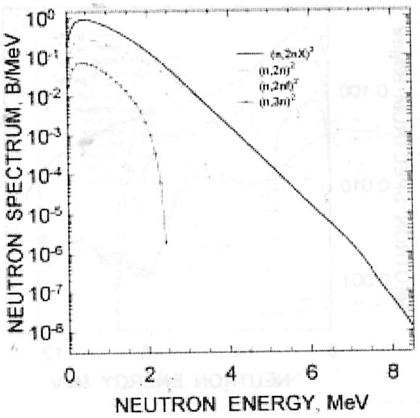

Figure 3: 2nd neutron spectrum of ^{235}U(n,F) at 14.7 MeV

i.e., ^{235}U(n,2nx)^1, multiplied by the fission probability of nuclide ^{234}U:

$$\frac{d\sigma^1_{n2nf}}{d\varepsilon} = \int_0^{E_n - B_n^{235}} \frac{d\sigma^1_{n2nx}}{d\varepsilon} \frac{\Gamma_f^{234}(E_n - B_n^{235} - \varepsilon - \varepsilon_1)}{\Gamma^{234}(E_n - B_n^{235} - \varepsilon - \varepsilon_1)} d\varepsilon_1 \qquad (3)$$

The hard-energy tail of the first neutron spectrum $\frac{d\sigma^1_{n2nf}}{d\varepsilon}$ of the ^{235}U(n,2nf) reaction would resemble the fission probability shape of ^{234}U nuclide.

Figure 5 shows (n,nf)^{1}and (n,2nf)^1 components of the first neutron spectrum ^{235}U(n,nx)^{1}at E_n ~14.7 MeV. Relative contributions of first neutron spectra of (n,xnf) reaction to the first neutron spectrum of ^{235}U(n,nx)^1 reaction are correlated with γ-emission/neutron/fission competition for the residual U nuclei, i.e., by the level density and fission barrier parameters of relevant fissioning and residual nuclei. (n,nf)^{1}and (n,2nf)^1 components

Shape of the (n,nf)^1 spectrum $\frac{d\sigma^1_{nnf}}{d\varepsilon}$ for ^{235}U(n,F) reaction is defined by the fission probability of ^{235}U nuclide. Figure 1 demonstrates that contribution of the (n,nf) second-chance fission reaction to the observed fission cross sections is rather flat above the relevant threshold E_{nnf}. However, sharp decrease of ^{235}U(n,nf)^1 reaction spectrum for emitted first neutron energies $\varepsilon \gtrsim E_n - B_f$ would be evidenced in measured prompt fission neutron spectrum (see below). The (n,2nf)^1 spectrum $\frac{d\sigma^1_{n2nf}}{d\varepsilon}$ contribution is systematically lower than that of (n,nf)^1 (see Fig. 5), however with the increase of the E_n up to ~20 MeV it might turn higher.

Exclusive second and third neutron spectra of the ^{235}U(n,2nf) and ^{235}U(n,3nf) reactions, are calculated as a double or triple integrals, starting from the ^{235}U(n,2nx)^2 and ^{235}U(n,3nx)^3, i.e. emission spectra of the second and third neutrons, respectively. First (n,2nf)^1 and second (n,2nf)^2 neutron spectra of the ^{235}U(n,2nf) reaction are defined to a large extent by the fission probability of the ^{234}U nuclide. First (n,3nf)^1, second (n,3nf)^2 and third (n,3nf)^3 neutron

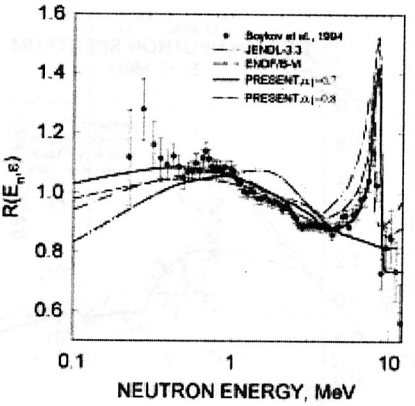

Figure 4: PFNS of ^{235}U(n,F) at 14.7 MeV

spectra of the ^{235}U(n,3nf) reaction are defined to a large extent by the fission probability of the ^{233}U nuclide. The details of the calculations are described in [2].

Figure 6 shows the $(n,2nf)^2$ component of the second neutron spectrum ^{235}U$(n,nx)^2$ at 14.7 MeV. Relative contribution of the second neutron spectrum of (n,2nf) reaction to the second neutron spectrum of ^{235}U$(n,2nx)^2$ reaction are correlated with γ-emission/neutron/fission competition for the residual U nuclei.

2.2 PFNS for multiple-chance fission

At incident neutron energies above emissive fission threshold and up to $E_n = 20$ MeV prompt fission neutron spectra $S(\varepsilon, E_n)$ are calculated as a superposition of (n,$x$nf) pre-fission neutron spectra $d\sigma^k_{nxnf}/d\varepsilon$ (x =1, 2, 3 or 4, k =1, 2...x) and post-fission spectra $S_{A+2-x}(\varepsilon, E_n)$ of neutrons, evaporated from fission fragments:

$$S(\varepsilon,E_n) = \widetilde{S}_{A+1}(\varepsilon,E_n) + \widetilde{S}_{A}(\varepsilon,E_n) + \widetilde{S}_{A-1}(\varepsilon,E_n) + \widetilde{S}_{A-2}(\varepsilon,E_n) =$$
$$\nu^{-1}(E_n)\{\nu_1(E_n)\cdot\beta_1(E_n)\cdot S_{A+1}(\varepsilon,E_n) + \beta_2(E_n)[\nu_2(E_n - \langle E_{nnf}\rangle)\cdot S_A(\varepsilon,E_n) + \frac{d\sigma^1_{nnf}}{d\varepsilon}]$$
$$+ \beta_3(E_n)[\nu_3(E_n - B^A_n - \langle E^1_{n2nf}\rangle - \langle E^2_{n2nf}\rangle)\cdot S_{A-1}(\varepsilon,E_n) + (\frac{d\sigma^1_{n2nf}}{d\varepsilon} + \frac{d\sigma^2_{n2nf}}{d\varepsilon})]+$$
$$\beta_4(E_n)[\nu_4(E_n - B^A_n - B^{A-1}_n - \langle E^1_{n3nf}\rangle - \langle E^2_{n3nf}\rangle - \langle E^3_{n3nf}\rangle)\cdot S_{A-2}(\varepsilon,E_n)$$
$$+ (\frac{d\sigma^1_{n3nf}}{d\varepsilon} + \frac{d\sigma^2_{n3nf}}{d\varepsilon} + \frac{d\sigma^3_{n3nf}}{d\varepsilon})]\}, \qquad (4)$$

$\widetilde{S}_{A+2-x}(\varepsilon, E_n)$ denote contributions to the observed prompt fission neutron spectra, which could be traced to multiple-chance fission reactions, $\langle E^k_{nxnf}\rangle$ is the $k-$th neutron average

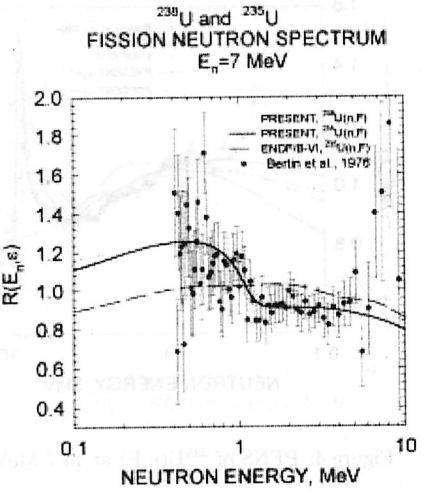

Figure 5: PFNS of ^{235}U(n,F) at 7 MeV

energy ($k \leq x$) of the (n,$x$nf)-reaction neutron spectrum $d\sigma^k_{nxnf}/d\varepsilon$. The calculation of S_{A+2-x} is described elsewhere [16]. The systematic [17] was used to estimate partial prompt neutron multiplicities ν_x below emissive fission threshold.

3 Measured PFNS data analysis

Figure 4 shows PFNS measured data for ^{235}U(n,F) reaction at E_n ~14.7 MeV and calculated PFNS. Data points as well as the calculated curves are shown relative to the Maxwell distributions with average energy $\langle E \rangle$ =2.136 MeV, PFNS of evaluated data files of ENDF/B-VI [12] (at E_n ~15 MeV) and JENDL-3.3 [18] (at E_n ~14 MeV) data libraries are also shown. Figure 5 shows the comparison of calculated PFNS, when available, at E_n =7 MeV. The variation of the (n,nf)[1] neutron contribution to the observed PFNS with the increase of $E_{th} \sim E_n - B_f$ energy is evident in present calculation. It looks like a wave, moving from the left (Fig. 5) to the right (Fig. 4) side of the plots.

Measured and calculated prompt fission neutron spectra at 14.7 MeV, i.e., above ^{235}U(n,2nf) emissive fission threshold, were reconciled with the same approach as it was done for the ^{238}U(n,F) and ^{232}Th(n,F) [2]. Considering only the influence of excitation energies on the emission process, $\alpha_{obs} \sim 0.9$ was estimated due to the pre-acceleration emission. We employ α_{obs} for ^{235}U(n,F) also for $E_n \leqslant$12 MeV, having in mind that it is at least a semi-empirical parameterization of measured PFNS data. We reproduced measured PFNS data for ^{238}U(n,F) and ^{232}Th(n,F) at E_n >12 MeV assuming that CMS energy per one nucleon E_{vo} is further reduced as:

$$\bar{E}_{\nu ij} = \alpha_1 \cdot \widetilde{E}_{\nu ij}. \tag{5}$$

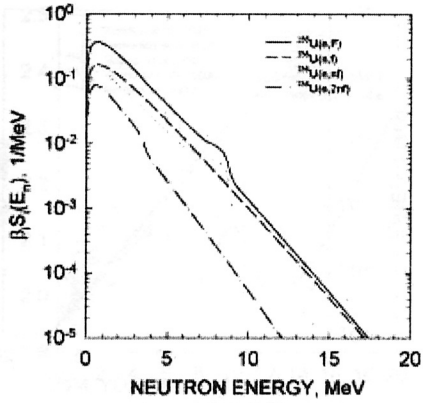

Figure 6: Multiple-chance components of ^{235}U(n,F) at 14.7 MeV

For ^{232}Th(n,F) and ^{238}U(n,F) we supposed that $\alpha_1 = 1$ for E_n <10 MeV and α_1 =0.8 for E_n >12 MeV and is linearly interpolated in between.

General trend of PFNS data for the ^{235}U(n,f) reaction at E_n =14.7 MeV (Fig. 4) is reproduced with α_1 =0.8, however a better fit is obtained with α_1 =0.7. For E_n =14.7 MeV (see Fig. 4) increase of E_{th} for (n,nf)[1] reaction spectra, as compared with E_n =7 MeV (Fig. 5) is reproduced. We might assume that change of the data shape around $\varepsilon \sim 3$ MeV is due to the sharp decrease of the first neutron spectrum contribution of (n,2nf)[1] reaction to the observed PFNS at E_n =14.7 MeV (see Fig. 4). Small excess of the soft neutrons with $\varepsilon \lesssim 0.5$ MeV is observed, but it is much lower than in previous evaluations of ENDF/B-VI [12] and JENDL-3.3 [18]. The peculiarities of the same nature were evidenced in case of ^{238}U(n,F) and ^{232}Th(n,F) PFNS data analysis [2].

Decomposition of the observed prompt fission neutron spectra into contributions of multiple-chance fission (see Eq. 9) allows to deconvolute the observed prompt fission neutron spectrum into contributions coming from non-emissive fission of ^{236}U nuclide $\widetilde{S}_{A+1}(E_n, \varepsilon)$, second-chance fission - (n,nf)-reaction neutrons and neutrons, evaporated from the fission fragments of ^{235}U nuclide $\widetilde{S}_A(E_n, \varepsilon)$, third-chance fission - (n,2nf)-reaction neutrons and neutrons, evaporated from the fission fragments of ^{234}U nuclide $\widetilde{S}_{A-1}(E_n, \varepsilon)$. Figure 6 shows contributions from the multiple-chance fission for ^{235}U(n,F) reaction at E_n =14.7 MeV.

In case of ^{235}U(n,F) reaction contribution from the first-chance fission at E_n =14.7 MeV is higher than those of second and third-chance fission reactions, only for $7 \lesssim \varepsilon \lesssim 8$ MeV the contribution of second-chance fission becomes higher than that of the first-chance fission. Contribution of the ^{235}U(n,nf)-reaction neutrons produces a wide peak in the observed PFNS (see Fig. 6). This second-chance fission contribution fades out at $\varepsilon \gtrsim 9$ MeV, at higher ε values mostly neutrons from fission fragments of fission of ^{236}U nuclide contribute to the $\widetilde{S}(E_n, \varepsilon)$. Contribution coming from the ^{235}U(n,2nf) fission reaction $\widetilde{S}_{A-1}(E_n, \varepsilon)$ is lower than those of ^{235}U(n,f) and ^{235}U(n,nf) reactions, i.e., $\widetilde{S}_{A+1}(E_n, \varepsilon)$ and $\widetilde{S}_A(E_n, \varepsilon)$, respectively. A flat step around $\varepsilon \sim 3$ MeV is due to the contribution of (n,2nf)[1], the first neutron of

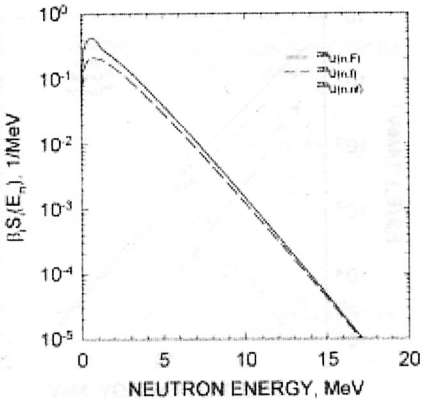

Figure 7: Multiple-chance components of ^{235}U(n,F) at 7 MeV

(n,2nf) reaction, it fades out at higher ε values as well. At higher E_n the same peculiarity in $\widetilde{S}_{A-2}(E_n, \varepsilon)$ might be observed, it might be due to the contribution of the first neutron of (n,3nf) reaction. The peculiarities, observed for the PFNS of E_n =14.7 MeV are much different from those, shown on Fig. 40 in paper by Madland an Nix [19], where the second-chance fission contributes mostly to the PFNS at E_n =14.7 MeV. That might be due to rather fast decrease of the first-chance fission contribution to the observed fission cross section, assumed by Madland an Nix [19] and adopted in the evaluation of ENDF/B-VI [12] (see Fig. 1).

At E_n =7 MeV contribution of the second-chance fission equals to that of the first-chance fission for $\varepsilon \lesssim 1$ MeV (see Fig 7), that is obviously due to the appreciable contribution of the pre-fission neutron. For higher emitted neutron energies ε the second-chance fission contribution is systematically lower than that of the first-chance fission. Actually, the excess of soft neutrons for PFNS of ^{235}U(n,F) at E_n =7 MeV was observed gas early as in 1975 [20] (see Fig.5). General trend of the measured data by Frehaut et al. [20] is quite compatible with present calculation.

Figure 8 compares average energies of PFNS $\langle E \rangle$, measured by Ethvignot et al. [4], previous experimental data [6, 21, 20, 22, 23] with evaluated data [18, 12, 24] and present calculations. Average energies $\langle E \rangle$ by Ethvignot et al. [4] were obtained by detecting emitted prompt fission neutrons with energies from ε =0.8 MeV to ε =7.5 MeV. The authors [4] claim to diminish the influence of the emitted energy cuts on the average energy estimates and provide the average over all emitted neutron energies. Indeed, the $\langle E \rangle$ by Ethvignot et al. [4] is rather close to the previous experimental estimates in the first plateau region and at E_n ~14.7 MeV [6]. However, the average energy defined by Frehaut et al. [20] at E_n = 7 MeV for emitted prompt fission neutrons with energies from ε =1 MeV to ε =10 MeV coincides with the data by Ethvignot et al. [4]. Figure 5 shows that pre-fission neutrons at E_n = 7 MeV influence the observed PFNS shape for $\varepsilon \lesssim 1$ MeV, i.e., the sensitivity to the lower detection threshold would be rather high. Figure 8 shows that the largest differences

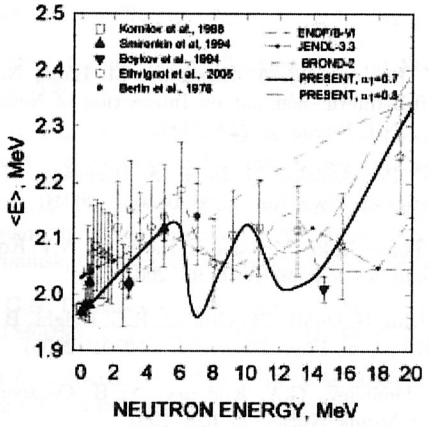

Figure 8: ^{235}U(n,F) PFNS average energy

of present calculations with the data by Ethvignot et al. [4] and ENDF/B-VI [12] calculation are in the vicinity of the ^{235}U(n,nf) and ^{235}U(n,2nf) reaction threshold.

4 Conclusion

Analysis of measured ^{235}U(n,F) cross section and PFNS data showed that a number of data peculiarities could be correlated with the influence of (n,$x$nf) pre-fission neutron spectra on the observed prompt fission neutron spectra. Predicted partial contribution of the second-chance fission ^{235}U(n,nf) to the observed fission cross section of ^{235}U(n,F) remains lower than that of the first-chance fission ^{235}U(n,f). Pre-fission ^{235}U(n,$x$nf) neutron emission lowers excitation energy of residual ^{235}U and ^{234}U nuclides. The spectra of pre-fission (n,$x$nf) are rather soft, as compared with the spectra of neutrons, emitted by primary fragments after scission of $^{236-x}$U nuclides. Combined effect of these peculiarities leads to the lowering of the average energy of the PFNS of ^{235}U(n,F) in the vicinity of ^{235}U(n,nf) and ^{235}U(n,2nf) reaction thresholds, while average energy of the PFNS of ^{235}U(n,F) increases with the incident neutron energy increase up to the ^{235}U(n,nf) reaction threshold. Structures in $\langle E \rangle$ of PFNS of ^{235}U(n,F), observed by Ethvignot et al. [4] in the vicinity of the first-chance and third-chance fission reactions are explained by the pre-fission neutron influence on PFNS.

Summarizing, we anticipate that partial (n,$x$nf) pre-fission neutron spectra for different target nuclei would be pronounced to a different extent in the observed PFNS for the target nuclides with different fissilities. Present estimates of the partial pre-fission neutron spectra, calculated simultaneously with consistent reproduction of ^{235}U(n,F) and ^{235}U(n,xn) reaction cross sections, might seem more reliable than various previous estimates, based on Weisscopf-Ewing approach [25], or more ambiguous phenomenological estimates of fission chance distributions, which are used in previous ^{235}U(n,F) PFNS analyses [19].

References

[1] V.M. Maslov, Yu.V. Porodzinskij, A. Hasegawa, M. Baba, N.V. Kornilov, A.B. Kagalenko, In: Proc.10th Intern. Seminar on Interaction of Neutrons with Nuclei, May 26-28, 2002, Dubna, JINR, Russia, p. 222, 2003.

[2] V.M. Maslov, Yu. V. Porodzinskij, M. Baba, A. Hasegawa, N.V. Kornilov, A.B. Kagalenko and N.A. Tetereva, Phys. Rev. C 69, 034607 (2004).

[3] V.M. Maslov, Yu.V. Porodzinskij, M.Baba, A. Hasegava, N.V. Kornilov, A.B. Kagalenko, N.A. Tetereva, Europhysics Journal, A 18, 93, 2003.

[4] T. Ethvignot, M. Devlin, H. Duarte, T. Granier, R.C. Haight, B. Morillon, R.O. Nelson, J.M. O'Donnel, D. Rochman, Phys. Rev. Lett., 052701 (2005).

[5] G.S. Boykov, V.D. Dmitriev, G.A. Kudyaev, Yu.B. Ostapenko, M.I. Svirin, G.N. Smirenkin, Physics of Atomic Nuclei, 53, 628, 1991.

[6] G.S. Boykov, V.D. Dmitriev, G.A. Kudyaev, V.M. Maslov, Yu.B. Ostapenko, M.I. Svirin, G.N. Smirenkin, Ann. Nucl. Energy, 21, 585 (1994).

[7] D. Hilscher and H. Rossner, Ann. Phys. Fr. 17, 471, 1992.

[8] M. Uhl and B. Strohmaier, IRK-76/01, IRK, Vienna ,1976.

[9] P.W. Lisowski , A. Gavron , W.E. Parker , J.L. Ullmann, S.J. Balestrini, A.D. Carlson, O.A. Wasson, N.W. Hill, Proc. Specialists' Meeting on Neutron Cross Section Standards for the Energy Region above 20 MeV, Uppsala, Sweden, May 21-23, 1991, p. 177, OECD, Paris, 1991.

[10] B. Leugers, S. Cerjacks et al., Proc. NEANDC/NEACRP Spec. Meeting on Fast Neutron Fission Cross Sections of ^{233}U, ^{235}U, ^{238}U and ^{239}Pu. ANL, June 28-30, 1976. ANL-76-90, 1976, 183.

[11] V.M. Maslov, Nucl.Phys. A, 743, (2004) 236.

[12] R.W.Roussin, P.G.Young, R. McKnight, Proc. Int. Conf. Nuclear Data for Science and Technology, Gatlinburg, USA, May 9-13, 1994, p. 692, J.K. Dickens (Ed.), ANS, 1994.

[13] V.M. Maslov, In: Nuclear Reaction data and Nuclear Reactors, Trieste, Italy, 2000, pp. 231-268, ICTP, 2001.

[14] C.K. Cline, Nucl. Phys. A195, 353 (1972).

[15] E. Gadioli, E. Gadioli Erba, P.G. Sona, Nucl. Phys. A217, 589 (1973).

[16] N.V. Kornilov, A.B. Kagalenko, F.-J. Hambsch, Physics of Atomic Nuclei, 62, 173 (1999).

[17] V.V. Malinovskij, Yadernye Konstanty, 2, 25, 1987.

[18] K. Shibata, T. Kawano, T. Nakagawa et al., J. Nucl. Sci. Technol., 39, 1125 (2002).

[19] D.C. Madland and J.R. Nix, Nucl. Sci. Eng., 81, 213, 1982.

[20] J. Frehaut, A. Bertin, R. Bois, Third All-Union Conf. on Neutron Physics, Kiev, 9-13 June, 1975, vol. 5, p. 349.

[21] N.V. Kornilov, A.B. Kagalenko, K.I. Zolotarev, Proc. VI Int. Seminar on Interaction of Neutrons with Nuclei, Dubna, May 13-16, 1998, Russia, E3-98-202, 1998.

[22] G.N. Lovchikova, A.M. Trufanov, M.I. Svirin, A.V. Polyakov,V.A. Vinogradov, V.D. Dmitriev, G.S. Boykov, In: Proceedings of the XIV International Workshop on Nuclear Fission Physics, Obninsk, October, 12-15, 2000, pp. 72-82, 2000.

[23] G.N. Smirenkin, G.N. Lovchikova, A.M. Trufanov, M.I. Svirin, A.V. Polyakov, V.A. Vinogradov, V.D. Dmitriev, G.S. Boykov, Yadernaya Fyzika, 59, 1934, 1996.

[24] G.V. Antcipov, A.B. Klepatskij, V.A. Konshin, V.M. Maslov et al., Evaluated data of ^{235}U. Minsk, Nauka i Technika, 1985 (in Russian).

[25] M.I. Svirin, G.N. Lovchikova, A.M. Trufanov, Yadernaya Fyzika, 60, 818 (1997).